Original Research Article

Investigating the Impact of Temperature on MgSe Structural, Optical and Electrical Features to Optimize its Use in Optoelectronics

Ernest O. Ojegu[1], Imosobomeh L. Ikhioya[2,*]

[1]*Department of Physics, Delta State University, Abraka, Delta State, Nigeria*
[2]*Department of Physics and Astronomy, University of Nigeria, Nsukka, 410001, Enugu State, Nigeria*

Citation E.O. Ojegu, I.L. Ikhioya. Investigating the Impact of Temperature on MgSe Structural, Optical and Electrical Features to Optimize its Use in Optoelectronics. *J. Eng. Ind. Res.* **2024**, 5 (1):16-26.

https://doi.org/10.48309/JEIRES.2024.5.2

Article info:
Submitted: 2024-02-22
Revised: 2024-04-27
Accepted: 2024-05-15
ID: JEIRES-2404-1118

Keywords:
MgSe; Bandgap energy; Resistivity; Conductivity; XRD

ABSTRACT

In this study, we used the electrochemical deposition technique to synthesize the MgSe material. The magnesium nitrate hexahydrate ($Mg(NO_3)_2.6H_2O$) and selenium (IV) oxide (SeO_2), are part of the electrochemical bath system. At a 2θ angle, MgSe material shows a diffraction angle of 15.669°. The diffraction peaks at 2θ = 15.669°, 16.452°, 17.426°, 23.489°, and 27.592° correspond, respectively, to the diffraction planes of 002, 100, 111, 112, and 212 of MgSe material. The film thickness decreased from 112.81 to 104.42 nm with an increase in the precursor temperature of MgSe. As the conductivity of the films increases from 1.01 to 1.17 S/m, the resistivity decreases from 98.09 to 85.42 ohm/cm. In the UV range, the films showed high transmittance, surpassing 70%. The films that underwent deposition at 50 °C demonstrated the highest transmittance, with an average of 72% in the visible and near-infrared spectrum. The reflectance value of every film that was deposited was over 15%. The films deposited had energy band gaps ranging from 1.75 to 2.56 eV. As the temperature increased, the energy band gap also increased. The bandgap energy range found in this study is perfect for absorbing solar energy radiation above 1.75 eV, making it ideal for solar cell absorber layers.

Introduction

The increasing interest in the growth of nanostructured semiconducting chalcogenides thin films is driven by their widespread use in scientific and technological domains. Wide band gap semiconductors like magnesium chalcogenides show promise for use in optoelectronic devices. The hygroscopic nature and unstable structure of MgSe make it poorly understood. MgSe is an important wide-bandgap semiconductor among different metal selenides, produced using complex physical methods [1,2]. Transition-metal chalcogenide semiconductors have gained widespread use in energy-related applications due to their exceptional water electro-catalysis activity.

*Corresponding Author: Imosobomeh L. Ikhioya (imosobomeh.ikhioya@unn.edu.ng)

Their magnetic and electronic features are widely recognized. The metal-chalcogen ratio in these transition metal chalcogenides can be varied extensively, allowing for fine-tuning of their electronic characteristics [3-8]. Transition-metal selenides show exceptional electrochemical activity compared to transition-metal oxides due to selenium's lower electronegativity than oxygen [9-14]. Therefore, substituting selenium with oxygen could cause a more flexible microstructure [15-19]. Magnesium selenide (MgSe) is a highly appealing binary semiconductor in the group II-IV family of metal selenide thin materials. At 0K, it has a wide band gap and can be found in various phases such as rock salt, wurtzite, and zinc blend. MgSe has found extensive applications in diverse fields such as microelectronics, photoelectric devices, solar selective coating, and catalysis. Because of its wide band gap, it can be utilized in high-power devices, high-temperature environments, and ultraviolet wavelength optics such as LEDs and cladding materials for ZnSe laser diodes [20-23]. Using the spray pyrolysis method, Sakhare *et al.* [1] fabricated nanocrystalline MgSe films by modifying the amount of spray solution. By investigating the quantity of spray solution, the study examined how it influenced the properties of MgSe thin films, including structure, electrical conductivity, morphology, and optical characteristics. The X-ray diffraction analysis revealed that the deposited MgSe possesses a cubic lattice and a preferred orientation (111). The optical analysis determined that the direct optical band gap of the MgSe deposition ranged from 2.45 to 2.75 eV, based on the amount of spray solution applied. The semiconducting properties of MgSe were revealed as its electrical resistivity decreased with increasing temperature. The spray solution quantity had an impact on electrical resistivity, activation energy, and optical band gap energy. The film's p-type conductivity was verified by measuring the thermo-emf using a temperature gradient. Ravindra and Sutjianto [5] used the periodic Hartree-Fock method to calculate the total energy of MgSe. Changes in unit cell volume were studied for the wurtzite, zinc-blende, and rocksalt phases. According to the results, MgSe typically forms a wurtzite phase under normal conditions. The transition from wurtzite to zinc-blende is unexpected, as zinc-blende has slightly higher energy at equilibrium volume. At around 60 GPa, the rocksalt phase undergoes a transition. The analysis of equilibrium volume reveals that the high-pressure phase of MgSe has an indirect minimum band gap. The electrodeposition technique was used in conducting this study. This method also helps decrease production expenses in large-scale production. The process is both inefficient and simple. Anti-reflective coatings, optoelectronic devices, and sensors are among the applications that use ECD-fabricated materials. This research aims to explore the impact of temperature on MgSe nanostructured material. The aim is to investigate how temperature affects the structural, optical, and electrical characteristics of MgSe to optimize its industrial applications.

Experimental

The electrochemical deposition technique was used to synthesize MgSe material. The $Mg(NO_3)_2.6H_2O$ and SeO_2, are part of the electrochemical bath system. Using a magnetic stirrer, we stirred the reaction bath. The power supply created the electric field (DC voltage), using conducting glass for the cathode and carbon and fluorine electrodes for the anode. Finally, we have successfully achieved uniform deposition of thin films using electrochemical deposition. The working electrode, coated with FTO and measuring 2.5 cm × 1.5 cm, was fragmented and cleaned using dishwashing liquid. To synthesize MgSe, 0.1 mol of $Mg(NO_3)_2.6H_2O$ and SeO_2 were mixed. The synthesis involves the use of a three-electrode system. The anode uses platinum, while the reference electrode comprises silver and silver chloride (Ag/AgCl), and the cathode is made of FTO (fluorine-doped tin oxide). The counter and reference electrodes were housed vertically in the beaker on the FTO-coated substrate. The synthesis required keeping a potentiostatic condition of -200 mV versus SCE for 5 seconds. The hand dryer was used to clean and dry the synthesized films. In the synthesis process, beakers were filled with target materials and equal amounts of precursors. A 20-minute annealing treatment was performed on the films

to ease internal stress. The properties of the synthesized materials were extensively analyzed using suitable tools to assess their optical, structural, elemental, and electrical characteristics.

Results

XRD analysis

The XRD pattern reveals the crystal structures of MgSe material, depicted in Figure 1. At a 2θ angle, MgSe material shows a diffraction angle of 15.669°. The diffraction peaks at 2θ = 15.669°, 16.452°, 17.426°, 23.489°, and 27.592° correspond respectively to the diffraction planes of 002, 100, 111, 112, and 212 of MgSe material. Equation 1 [24] was used to determine the size of the material's crystallites.

$$D = \frac{k\lambda}{\beta cos\theta} \quad (1)$$

Where, k = 0.9, λ = 0.12406 nm (wavelength of X-ray source), and β = FWHM in radians. The calculation of the crystallite size of MgSe material is presented in Table 1. Temperature is a key factor in determining the grain size of MgSe. Higher temperatures lead to larger grain sizes by promoting atom mobility and reducing nucleation barriers. The temperature range can affect grain size in various ways. For instance, the temperature increase can cause the grain size of MgSe to accumulate, especially within the range of 40-50 degrees. By adjusting the processing temperature, the grain size of MgSe increases. The application of heat and mechanical force during thermos-mechanical processing can impact the grain size and other properties of a material. Temperature influences the lattice spacing of MgSe. The lattice spacing expands as the temperature goes up. The increased vibration of atoms causes the expansion of the lattice at higher temperatures.

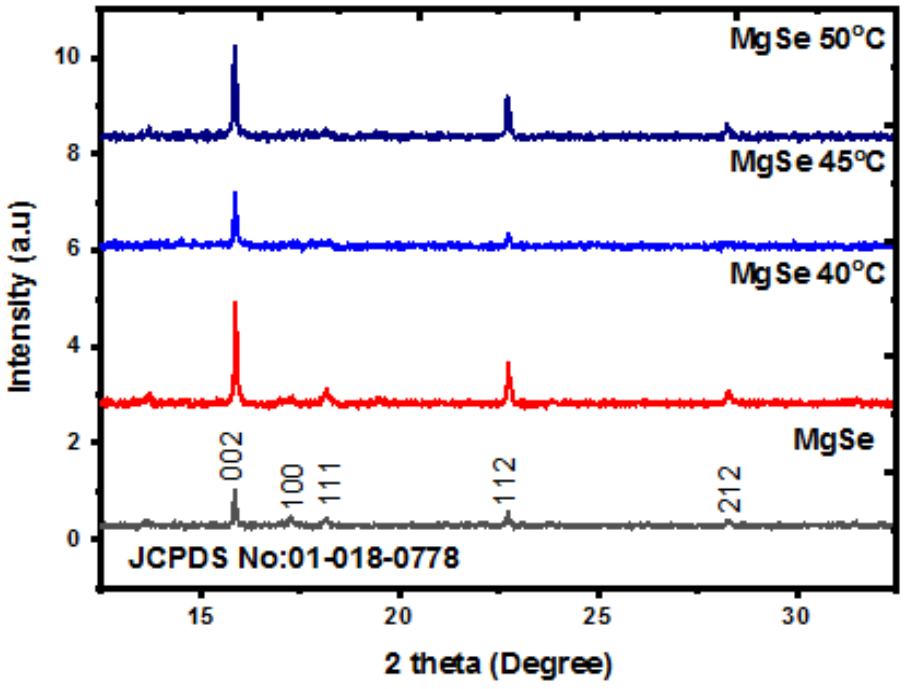

Figure 1: XRD pattern of MgSe

Table 1: Structural values of MgSe material

Films	2θ (degree)	d (spacing) Å	(Å)	(β)	(hkl)	(D) nm	σ (lines/m^2 x 10^{15})
MgSe	15.669	5.654	9.794	0.288	002	0.486	1.287
	16.452	5.387	10.774	0.286	100	0.490	1.267
	17.426	5.088	10.176	0.283	111	0.496	1.237
	23.489	3.786	8.467	0.281	112	0.504	1.197
	27.592	3.232	7.917	0.280	212	0.510	1.169
MgSe 40 °C	15.966	5.550	9.613	0.228	002	0.614	8.065
	16.818	5.270	10.541	0.226	100	0.620	7.907
	17.646	5.025	10.050	0.223	111	0.629	7.682
	23.919	3.719	8.317	0.221	112	0.641	7.394
	27.668	3.223	7.896	0.220	212	0.649	7.219
MgSe 45 °C	15.966	5.550	9.613	0.238	002	0.588	8.788
	16.818	5.270	10.541	0.236	100	0.594	8.622
	17.646	5.025	10.050	0.233	111	0.602	8.386
	23.919	3.719	8.317	0.231	112	0.614	8.079
	27.668	3.223	7.896	0.230	212	0.621	7.890
MgSe 50 °C	15.966	5.550	9.613	0.248	002	0.565	9.542
	16.818	5.270	10.541	0.246	100	0.570	9.369
	17.646	5.025	10.050	0.243	111	0.577	9.121
	23.919	3.719	8.317	0.241	112	0.588	8.794
	27.668	3.223	7.896	0.240	212	0.595	8.591

Resistivity and conductivity of MgSe material

In Table 2, we present the electrical analysis of MgSe materials. The film thickness decreased from 112.81 to 104.42 nm with an increase in the precursor temperature of MgSe. As the conductivity of the films increases from 1.01 to 1.17 S/m, the resistivity decreases from 98.09 to 85.42 ohm/cm. As the film thickness decreases, Figure 2 depicts the relationship between resistivity and conductivity in a semiconductor material. The improved conductivity of synthesized materials enables the development of more efficient solar device components. The resistivity and conductivity of MgSe change with temperature. The relationship between temperature and resistivity is inverse, while conductivity is directly proportional. The enhanced thermal energy results in greater electron mobility, leading to improved electrical conductivity in the material. At temperatures between 40-50 °C, the resistivity and conductivity of MgSe are affected, resulting in a decrease in film thickness. However, as the temperature rises, the resistivity of MgSe decreases as its conductivity increases. Temperature has a significant impact on the resistivity and conductivity of MgSe, as indicated by these studies. Higher temperatures lead to lower resistivity and higher conductivity.

2024, Volume 5, Issue 1

Table 2: Electrical properties of MgSe nanostructured material

Samples	T (nm)	ρ (Ω.cm) × 108	σ (S/m) × 106
MgSe	112.81	98.09	1.01
MgSe 40 oC	109.33	92.53	1.08
MgSe 45 oC	108.65	89.61	1.11
MgSe 50 oC	104.42	85.42	1.17

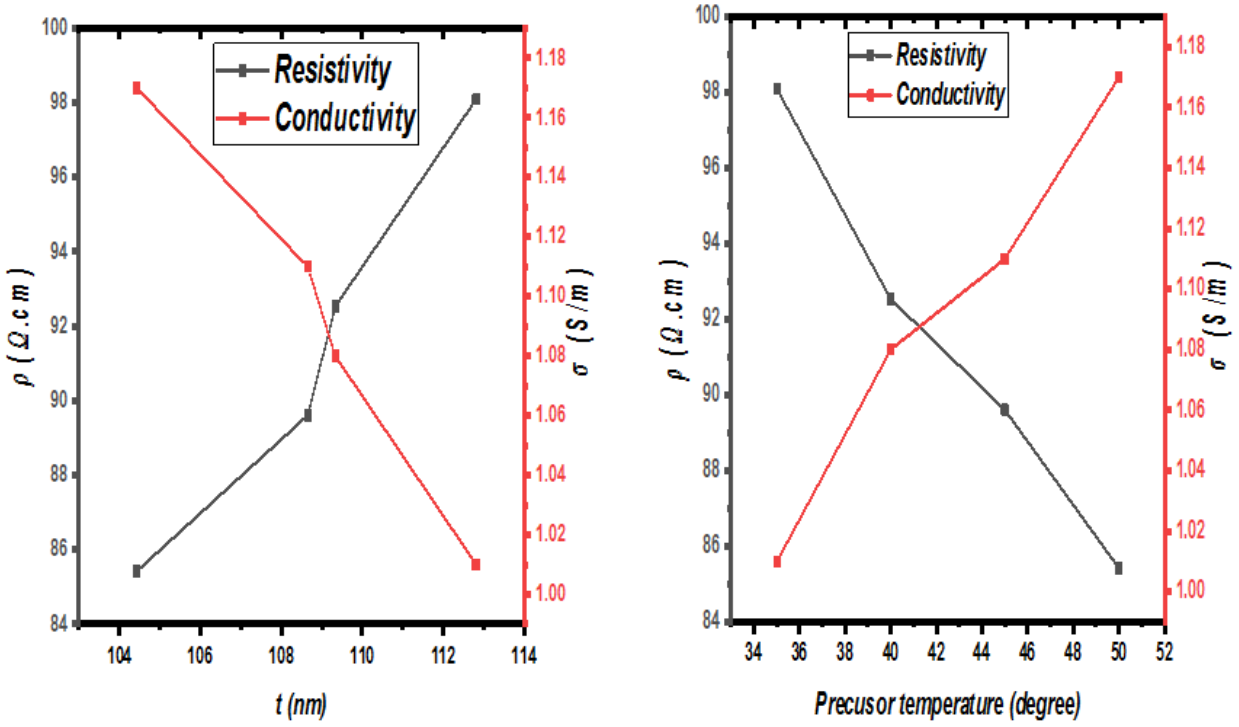

Figure 2: Resistivity and conductivity of MgSe

Optical analysis

$$T = 10^{-A} \quad (2)$$

$$R = 1 - (A + T) \quad (3)$$

Where, A = Absorbance, T = Transmittance, and R = Reflectance [17-19].

Figure 3 displays the absorbance of MgSe materials. The absorbance of MgSe decreases as the wavelength gets closer to the VIS-IR region. The absorbance of the MgSe material deposited at room temperature surpassed all others across the entire spectrum. Due to the precursor temperature, there was a reduction in the absorbance spectra. The increase in the size of MgSe may be due to the rise in the crystallite peak observed in the XRD pattern. These films have excellent absorbance in the near-infrared and visible spectrum, making them perfect for creating p-n junctions in solar cells and other photovoltaic uses. The MgSe absorbance changes with temperature variations. As the temperature rises, the absorbance decreases. The temperature also affects the thermal conductivity of MgSe. The conductivity rises as temperatures increase. The temperature-dependent properties of MgSe make it a promising material for thermoelectric applications. Equation 2 and Figure 4 are used to derive the transmittance values from the absorbance values. The results reveal that MgSe possesses greater transmittance in the VIS-IR

spectrum, suggesting its suitability for photovoltaic devices. In the UV range, the films showed high transmittance, surpassing 70%. The films that underwent deposition at 50 °C demonstrated the highest transmittance, with an average of 72% in the visible and near-infrared spectrum. The transmittance of MgSe material varies with temperature. Temperature influences the transmittance of MgSe, causing a decrease in transmittance at higher temperatures. With increasing temperature, the bandgap of MgSe decreases, enabling greater absorption of photons. Figure 5 shows that all the films deposited had very low reflectance values, as evaluated using Equation 3. The reflectance values slightly increased from ultraviolet to visible, remaining relatively constant in the visible and near-infrared regions. The reflectance value of every film that was deposited was over 15%. Window layers in photovoltaic applications benefit from their low reflectance, especially in the Visible region. Temperature impacts the reflectance of MgSe, causing lower reflectance at higher temperatures. The atoms in MgSe vibrate more due to increased thermal energy, disrupting their orderly arrangement and decreasing light reflection. The MgSe reflectance, which varies with temperature, has potential uses in multiple industries. It has potential applications in optical devices like temperature sensors or optical filters that need precise control over light reflection. Figure 6 depicts the correlation between $(\alpha hv)^2$ and hv in MgSe material. The energy band gaps of the material were determined by extrapolating the graph's linear region to $(\alpha hv)^2 = 0$. The films deposited had energy band gaps ranging from 1.75 to 2.56 eV. As the temperature increased, the energy band gap also increased. The bandgap energy range found in this study is perfect for absorbing solar energy radiation above 1.75 eV, making it ideal for solar cell absorber layers. As the temperature rises, the bandgap energy of MgSe also increases. Electrons are thermally excited from the valence band to the conduction band, causing this increase in the bandgap energy of MgSe. Scientists have employed techniques like photoluminescence and absorption spectroscopy to experimentally measure the temperature dependence of the bandgap energy of MgSe. Increasing temperature has a direct relationship with the bandgap energy, resulting in a linear increase. Density functional theory (DFT) was used to calculate theoretically the temperature dependence of the bandgap energy of MgSe. The calculations reveal that the anharmonic effects of lattice vibrations cause the rise in bandgap energy at higher temperatures. The energy band gap of MgSe increases with rising temperature. The increase in thermal vibrations of the atoms causes the potential seen by the electrons to rise, resulting in an increased band gap. The band gap of MgSe shows a non-linear relationship with temperature at low temperatures. As the temperature rises, it transitions from slow variation to near linearity. The estimated band gap of MgSe at non-zero temperature is approximately 1.75 eV. Thin films grown via electrochemical deposition have shown values between 2.15 and 2.56 eV. The energy bandgap of MgSe increases alongside rising temperatures. The lattice expansion and electron-phonon interactions are responsible for this phenomenon, as they weaken the interatomic bonds and raise the energy needed to excite electrons from the valence band to the conduction band.

The bandgap of MgSe has been investigated for its temperature dependence using both theoretical calculations and experimental measurements. Experimental observations align with DFT simulations that show a rise in the bandgap as the temperature increases. The Varshni Equation can express the relationship between temperature and bandgap in MgSe: $Eg(T) = Eg(0) - \alpha T^2 / (\beta + T)$. The expansion of the MgSe lattice is caused by increased atomic vibrations as the temperature rises. The material's physical properties, like density and thermal conductivity, are impacted by this expansion. The energy band gap of MgSe increases with rising temperature. The reason for this is that the rise in thermal energy stimulates electrons to higher energy levels, creating a larger gap between the valence and conduction bands.

2024, Volume 5, Issue 1

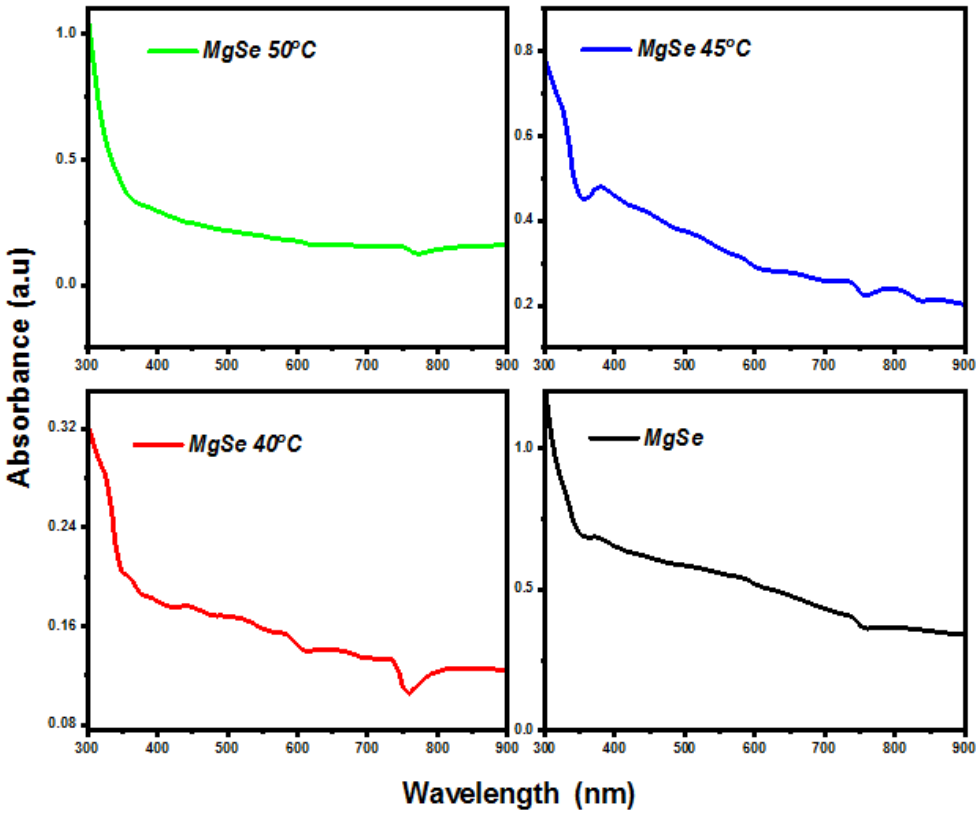

Figure 3: Absorbance of MgSe

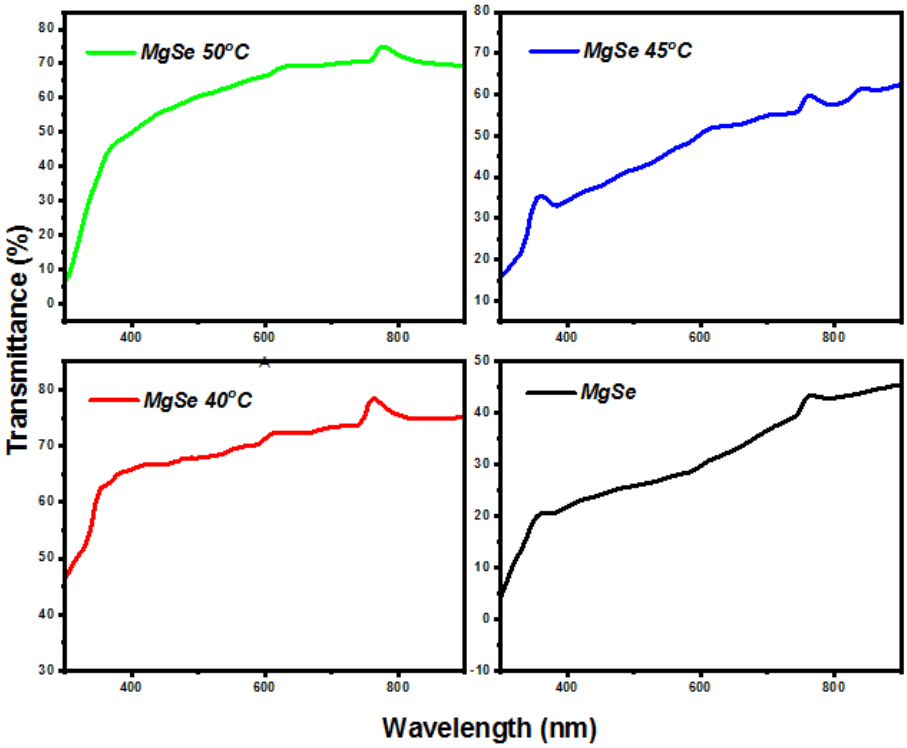

Figure 4: Transmittance of MgSe

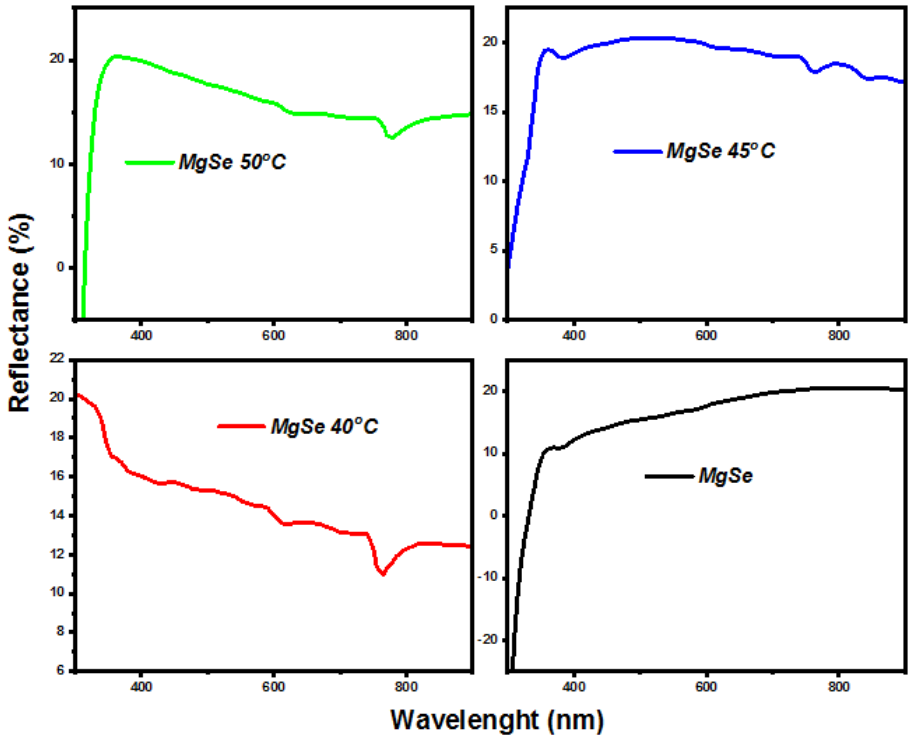

Figure 5: MgSe reflectance

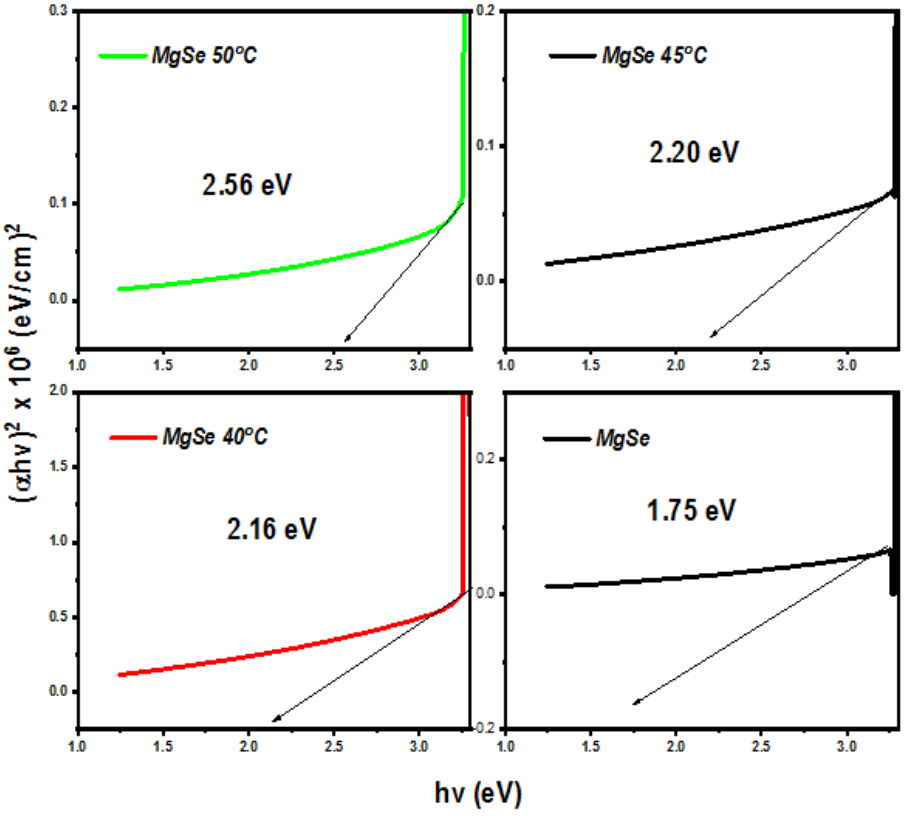

Figure 6: Bandgap energy of MgSe

2024, Volume 5, Issue 1

Conclusion

We have successfully used the electrochemical deposition technique to synthesize the MgSe material. The absorbance of the MgSe material deposited at room temperature surpassed all others across the entire spectrum. Due to the precursor temperature, there was a reduction in the absorbance spectra. The increase in the size of MgSe may be due to the rise in the crystallite peak observed in the XRD pattern. At a 2θ angle, MgSe material shows a diffraction angle of 15.669°. The diffraction peaks at 2θ = 15.669°, 16.452°, 17.426°, 23.489°, and 27.592° correspond, respectively, to the diffraction planes of 002, 100, 111, 112, and 212 of MgSe material. The film thickness decreased from 112.81 to 104.42 nm with an increase in the precursor temperature of MgSe. As the conductivity of the films increases from 1.01 to 1.17 S/m, the resistivity decreases from 98.09 to 85.42 ohm/cm. In the UV range, the films showed high transmittance, surpassing 70%. The films that underwent deposition at 50 °C demonstrated the highest transmittance, with an average of 72% in the visible and near-infrared spectrum. The reflectance value of each deposited film was over 15%. The films deposited had energy band gaps ranging from 1.75 to 2.56 eV. As the temperature increased, the energy band gap also increased. The bandgap energy range found in this study is perfect for absorbing solar energy radiation above 1.75 eV, making it ideal for solar cell absorber layers.

Authors' Contributions

Ernest O. Ojegu and Imosobomeh L. Ikhioya: Conceptualization, methodology, and data curation, Imosobomeh L. Ikhioya: Data collection, first-draft writing, reviewing, software, and editing, investigation, and visualization. All authors approved the submission.

Conflict of Interest

The authors declare no personal or financial conflicts that may have impacted the research in question.

Data Availability

Data can be accessed by making a request.

Acknowledgments

We extend our thanks to all the authors for their financial support, which contributed to the success of the research.

ORCID

Imosobomeh L. Ikhioya
https://orcid.org/0000-0002-5959-4427

Reference

[1]. Y.S. Sakhare, N.R. Thakare, A.U. Ubale, Influence of quantity of spray solution on the physical properties of spray-deposited nanocrystalline MgSe thin films, *Physical and Mathematical Sciences.*, **2016**, *2*, 29-40. [Google Scholar], [Publisher]

[2]. A.U. Ubale, Y.S. Sakhare, Thickness dependent physical properties of chemically deposited nanocrystalline MgSe thin films deposited at room temperature by solution growth method, *Materials Science in Semiconductor Processing*, **2013**, *16*, 1769-1774. [Crossref], [Google Scholar], [Publisher]

[3]. D. Sofronov, Y. Zagoruiko, N. Kovalenko, A. Gerasimenko, V. Baumer, P. Mateychenko, A. Mamalis, S. Lavrynenko, Microwave synthesis of Mgse for Zn1-xMgxse crystal growth, *Materials and Manufacturing Processes*, **2013**, *28*, 944-946. [Google Scholar], [Publisher]

[4]. Y. Selmani, H. Labrim, A. Jabar, L. Bahmad, Thermoelectric properties of Mg-doped mercury selenide HgSe, *International Journal of Modern Physics B*, **2023**, 2450334. [Crossref], [Google Scholar], [Publisher]

[5]. R. Pandey, A. Sutjianto, Study of structural phase transition in MgSe, *Solid State Communications*, **1994**, *91*, 269-271. [Crossref], [Google Scholar], [Publisher]
[6]. K. Udofia, I. Lucky, Electrical properties of electrodeposited lead selenide (PbSe) thin films, *Asian Journal of Physical and Chemical Sciences*, **2018**, *5*, 1-7. [Google Scholar], [Publisher]
[7]. K.I. Udofia, I. Ikhioya, D.N. Okoli, A.J. Ekpunobi, Impact of doping on the physical properties of PbSe chalcogenide material for photovoltaic application, *Journal of Medicinal and Nanomaterials Chemistry*, **2023**, *5*, 135-147. [Crossref], [Publisher]
[8]. I. Ikhioya, N.I. Akpu, E. Onoh, S.O. Aisida, I. Ahmad, M. Maaza, F. Ezema, Impact of precursor temperature on physical properties of molybdenum doped nickel telluride metal chalcogenide material, *Journal of Medicinal and Nanomaterials Chemistry*, **2023**, *5*, 156-167. [Crossref], [Publisher]
[9]. S.O. Samuel, Z.J. Timothy, C.K. Ojoba, I.L. Ikhioya, Temperature's impact on the physical properties of rare earth element doped SrS for optoelectronic use, *Journal of Engineering in Industrial Research*, **2023**, *4*, 147-156. [Crossref], [Google Scholar], [Publisher]
[10]. M. Yin, S. O'Brien, Synthesis and characterization of nanostructured nickel diselenide $NiSe_2$from the decomposition of nickel acetate, $(CH_3CO_2)_2Ni$, *Journal of Nanomaterials*, **2014**, *2014*, 503676. [Crossref], [Google Scholar], [Publisher]
[11]. S. Zan, W. Zhang, H. Li, R. Wang, S. Qi, NiSe@$MoSe_2$ foam: Synthesis, characterization and microwave absorption investigation, *Journal of Materials Science: Materials in Electronics*, **2023**, *34*, 56. [Crossref], [Google Scholar], [Publisher]
[12]. B. Zhao, J.W. Liu, Y.R. Yin, D. Wu, J.L. Luo, X.Z. Fu, Carbon nanofibers@NiSe core/sheath nanostructures as efficient electrocatalysts for integrating highly selective methanol conversion and less-energy intensive hydrogen production, *Journal of Materials Chemistry A*, 2019, *7*, 25878–25886.[Crossref], [Google Scholar], [Publisher]
[13]. I. Rufus, A. Peter, S.O. Aisida, I.L. Ikhioya, Influence of manganese molarity incorporation on manganese silver sulphide semiconductor material for photovoltaic applications, *Results in Optics*, **2023**, *12*, 100464. [Crossref], [Google Scholar], [Publisher]
[14]. B. Ye, X. Cao, Q. Zhao, J. Wang, Coelectrodeposition of NiSe/ZnSe hybrid nanostructures as a battery-type electrode for an asymmetric supercapacitor, *Journal of Physical Chemistry C*, **2020**, *124*, 21242–21249. [Crossref], [Google Scholar], [Publisher]
[16]. Y.H. Zhang, H.Y. Yan, J.T. Zhao, D.D. Wang, S.H. Luo, Q. Wang, X. Liu, Hydrothermal synthesis of $NiSe_2$ octahedral structure and sodium ion storage performance, *Journal of Electroanalytical Chemistry,* **2023**, *943*, 117596. [Crossref], [Google Scholar], [Publisher]
[17]. N. Moloto, M.J. Moloto, N.J. Coville, S. Sinha Ray, Optical and structural characterization of nickel selenide nanoparticles synthesized by simple methods, *Journal of Crystal Growth*, **2009**, *311*, 3924-3932. [Crossref], [Google Scholar], [Publisher]
[18]. L.L. Pan, G.Y. Li, J.S. Lian, Structural, optical and electrical properties of cerium and gadolinium doped CdO thin films, *Applied Surface Science*, **2013**, *274*, 365-370. [Crossref], [Google Scholar], [Publisher]
[19]. F. Jiang, Q. Liao, G. Fan, C. Xiong, X. Peng, C. Pan, N. Liu, MOCVD growth of MgSe thin films on GaAs substrates, *Journal of Crystal Frowth*, **1998**, *183*, 289-293. [Crossref], [Google Scholar], [Publisher]
[20]. O. Ojegu, O. Omamoke, Optical properties of the anatase phase of titanium dioxide thin films prepared by electrostatic spray deposition, *Nigerian Journal of Science and Environment*, **2020**, *18*. [Google Scholar]
[21]. S. Burnett, R. Ferns, D.B. Cordes, A.M. Slawin, T. van Mourik, A. Stasch, Low-coordinate magnesium sulfide and selenide complexes, *Inorganic Chemistry*, **2023**, *62*, 16443-16450. [Crossref], [Google Scholar], [Publisher]
[22]. S.R. Alharbi, A.F. Qasrawi, In/MgSe Terahertz filters with enhanced optical conduction

2024, Volume 5, Issue 1

and light absorption, *Journal of Electronic Materials*, **2023**, *52*, 3613-3621. [Crossref], [Google Scholar], [Publisher]

[23]. H. Yao, X. Ning, H. Zhao, A. Hao, and M. Ismail, Effect of Gd-doping on structural, optical, and magnetic properties of $NiFe_2O_4$As-prepared thin films via facile sol-gel approach, *ACS Omega*, **2021**, *6*, 6305–6311. [Crossref], [Google Scholar], [Publisher]

[24]. R. Muthaiah, J. Garg, Thermal conductivity of magnesium selenide (MgSe)–A first principles study, *Computational Materials Science*, **2021**, *198*, 110679. [Crossref], [Google Scholar], [Publisher]